

Crossover from static to thermal layer undulations in finite-size liquid-crystalline films

R. E. Geer and R. Shashidhar

Center for Bio/Molecular Science and Engineering, Code 6900, Naval Research Laboratory, Washington, D.C. 20375

(Received 14 July 1994)

A quantitative study of the crossover from static to thermally dominated layer undulations in a liquid-crystalline film is presented. Off-specular x-ray scattering from Langmuir-Blodgett multilayers of liquid-crystalline monomer-polymer mixtures reveals that the amplitude of smectic layer undulations is dominated by static roughness for low monomer concentrations. With increasing monomer concentration, the contribution due to thermally induced undulations increases rapidly with a concomitant decrease in the in-plane correlation length associated with the layer undulation correlation function.

PACS number(s): 61.30.Eb, 68.18.+p, 68.65.+g, 61.41.+e

Smectic-A and smectic-C liquid crystals are characterized by quasi-long-range positional order (layer order) in one dimension and short-range positional order (fluidity) in the other two dimensions [1]. The amplitude of thermally induced layer undulations for such a system diverges logarithmically with sample size [2]. The roughness of a bounding surface can also induce layer undulations, albeit static in nature [1]. Thus the layer undulations of a finite-size smectic-A (or smectic-C) sample result from a combination of thermally induced fluctuations and static undulations induced by surface roughness. Generally, for low molecular weight thermotropic liquid crystals, the thermal fluctuations are large and overwhelm the static undulations [2]. Recently it was shown that in the case of siloxane-based polymeric liquid-crystal materials, the flexible siloxane backbone separates the mesogenic components of adjacent layers leading thereby to a high degree of layer order defined by the backbone [3]. This, in turn, leads to a significant quenching of the thermal fluctuations of the layer and makes it possible to study quantitatively the nature of static undulations [4]. However, a study of the crossover from predominantly static to predominantly thermal undulations has not been carried out for any liquid-crystal system so far.

In this paper we present a quantitative study of the crossover from primarily static to thermally dominated undulations from Langmuir-Blodgett films deposited from monolayers of liquid-crystal polymer-monomer mixtures. By analyzing the off-specular diffuse x-ray scattering, which is extremely sensitive to layer and interfacial disorder [5,6], it is shown that increases in the monomer concentration result in a concomitant increase in the root-mean-square roughness of the smectic layers. Also, the in-plane correlation length associated with the average layer undulation correlation function decreases rapidly with increased monomer concentration.

The materials studied are mixtures of a siloxane-based side-chain copolymer [7] with its own (unattached) side group, i.e., monomeric, mesogen. The phase transition temperatures of the mixtures have been reported earlier [8]. The important feature relevant to this study is that they all exhibit the ferroelectric smectic-C* phase at ambient temperatures. This permits the formation of Langmuir monolayers of mixed systems. Subsequent transfer of these monolayers to a silicon wafer (hydrophobized with a chemisorbed silane

film) results in Langmuir-Blodgett multilayers. The x-ray beam (Rigaku RU-200 rotating anode source) used for diffraction was collimated by two tantalum slits placed between the sample and the monochromator (graphite), and two more between the sample and the scintillation detector. The in-plane resolutions are $\Delta q_x = 8 \times 10^{-4} \text{ \AA}^{-1}$ and $\Delta q_z = 1.1 \times 10^{-3} \text{ \AA}^{-1}$. The out-of-plane resolution, $\Delta q_y \approx 0.2 \text{ \AA}^{-1}$, was determined primarily by the slit height.

Each film consisted of 30 transferred monolayers. Figure 1 shows the specularly reflected x-ray intensity from films of 10%, 20%, 30%, and 50% monomer (mole percentage). The smectic layer spacing of 40.2 Å as determined from the first Bragg reflection is roughly independent of concentration,

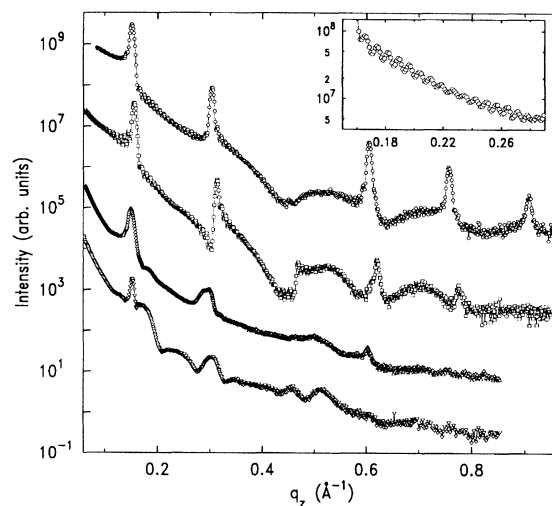


FIG. 1. Specular reflectivity from Langmuir-Blodgett multilayers of liquid-crystalline copolymer-monomer mixtures: open circles denote 10% monomer mole percentage; squares denote 20%; triangles denote 30%; and inverted triangles denote 50%. Data have been offset for clarity. As the monomer concentration increases the number and strength of the Bragg reflections decrease. The broad features in the 30% and 50% data are discussed in the text. Solid lines are a guide to the eye. Inset: subsidiary maxima between the first and second Bragg reflections for the 10% polymer-monomer mixture.

showing a 1.2 Å increase for the 10% mixture only. The width of the subsidiary maxima present between the Bragg reflections (see inset of Fig. 1) $w = 2\pi/D$ (where D is the film thickness), yields thicknesses of 810 ± 8 Å, 835 ± 10 Å, 733 ± 16 Å, and 765 ± 14 Å for the 10%, 20%, 30%, and 50% films, respectively.

Similar to pure copolymer films [9], the specular reflectivity for the 10% sample shows five Bragg reflections (the absence of the third order reflection is also seen in films of the pure copolymer and in the bulk copolymer, which is the result of a zero in the molecular form factor). In the 20% film the highest order reflection is lost. For 30% monomer mole percentage the fourth order is significantly reduced, and the second order broadened. For the 50% mixture only the primary Bragg reflection is sharp enough to be associated with smectic domains spanning the film thickness. Broad oscillations are also evident in the scattered intensity at $q_z \approx 0.3$ and 0.5 for the 30% and 50% films. The presence of both sharp and broad features suggest a coexistence of a thin (≈ 60 Å as determined from the width of the peaks) layered region near the film surface with much thicker smectic domains. Such a coexistence of separate surface and bulk regions has previously been seen in spin-cast films of liquid-crystalline monomers [10].

The reduction in the intensity and number of Bragg reflections with increasing monomer concentration is due to a decrease in the smectic layer order. This is not unexpected since most monomeric smectic-A and smectic-C liquid crystals only possess one or two Bragg reflections from the smectic mass density wave due to large thermally induced layer undulations [2]. This is the case for the 50% film which exhibits only a single sharp Bragg reflection. Conversely, for pure copolymer and low percentage ($\approx 10\%$) monomer films, the large layer compressive elastic constants suppress thermal fluctuations and the layer disorder in these films is dominated by roughness propagating from the substrate [4]. To investigate the crossover between these two regimes we examine the off-specular scattering in the vicinity of the first Bragg reflection. These data, shown in Fig. 2, consist of sharp specular peaks superposed on broad diffuse scattering.

Inspection of the specular portion of the scattering in Fig. 2 reveals an increase in the film mosaicity with monomer concentration. The width of these specular peaks increases from approximately 0.03° for the 10% and 20% data to

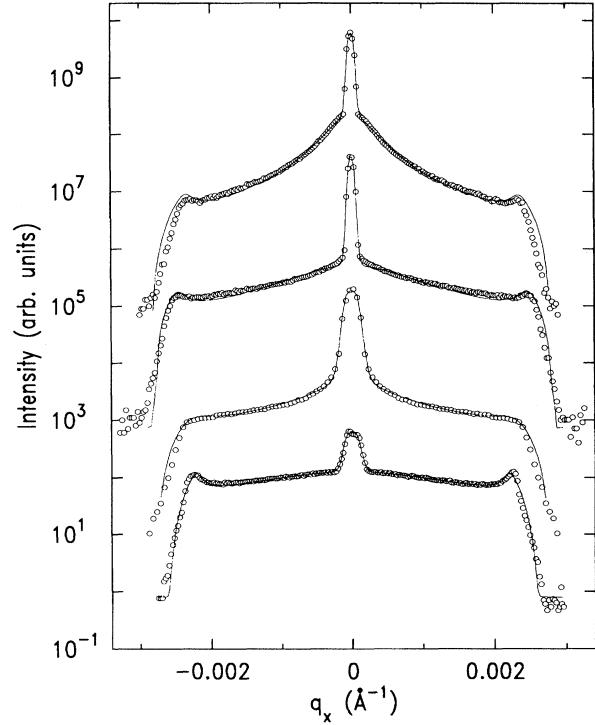


FIG. 2. Off-specular scattering across the first Bragg reflection of the (from top to bottom) 10%, 20%, 30%, and 50% films. With increasing monomer concentration the diffuse scattering becomes broader. Also note the increased mosaicity in the 30% and 50% films. Solid lines represent best fits to the model described in the text.

0.07° and 0.08° for the 30% and 50% monomer concentrations, respectively. The line shape of the diffuse scattering is also affected, becoming nearly flat at high concentrations. For a quantitative description of this line shape, recall that the scattered intensity $I(\mathbf{q})$ from any multilayer structure (assuming no in-plane density modulation and ignoring refraction) is given by [11]

$$I \cong \frac{I_0}{q_z^2 \sin(\alpha) \sin(\beta)} \int \int dz' dz \frac{d\rho(z)}{dz} \frac{d\rho^*(z')}{dz'} \int \int dx dy (e^{q_z C(x,y,z-z')} e^{-i\mathbf{q}_\perp \cdot \mathbf{r}_\perp} e^{-iq_z(z-z')}), \quad (1)$$

where α and β are the incident and exit angles, respectively, $\rho(z)$ is the electron density profile normal to the surface, \mathbf{r}_\perp is the in-plane position vector, and $C(x,y,z-z')$ is the layer roughness correlation function $\langle z(\mathbf{r})z(0) \rangle$. The low resolution, Δq_y , effectively reduces the in-plane integration to the x direction only.

For smectic films on solid supports the above correlation function is dependent upon both static and thermally induced

layer undulations. Static undulations due to the penetration of substrate roughness decay exponentially from the substrate surface with a characteristic length $L \equiv q_x^{-2}(B/K)^{1/2}$ [4,12]. From the data in Fig. 2 note that $|q_x| \leq 0.002 \text{ \AA}^{-1}$. Thus L varies from $1.25 \times 10^5 \text{ \AA}$ for the case of the pure copolymer ($B \approx 2.5 \times 10^9 \text{ dyn/cm}^2$, $K \approx 1 \times 10^{-6} \text{ dyn}$) to $1.23 \times 10^3 \text{ \AA}$ for monomeric materials ($B \approx 2.5 \times 10^7 \text{ dyn/cm}^2$, $K \approx 1 \times 10^{-6} \text{ dyn}$). Both are significantly greater than the film

TABLE I. Model parameters from best fits to the data in Fig. 2. Both $\bar{\sigma}$ and $\bar{\xi}$ vary monotonically with increasing monomer mole fraction. \bar{h} does not vary, with the exception of the 30% film.

| Monomer mole fraction | $\bar{\sigma}$ (Å) | $\bar{\xi}$ (Å) | \bar{h} |
|-----------------------|--------------------|-----------------|-----------------|
| 0.10 | 3.0 ± 0.2 | 3014 ± 22 | 0.5 ± 0.05 |
| 0.20 | 3.2 ± 0.2 | 1141 ± 29 | 0.5 ± 0.05 |
| 0.30 | 4.0 ± 0.2 | 798 ± 32 | 0.35 ± 0.05 |
| 0.50 | 7.0 ± 0.3 | 592 ± 45 | 0.5 ± 0.05 |

thickness. Thus *substrate roughness is expected to penetrate the film thickness completely, regardless of the composition.*

We expect thermally induced layer undulations, however, to be more sensitive to the magnitude of the elastic constants and hence to the composition. The layer undulation correlation function has been calculated by Holyst [13] in the case of freely suspended liquid-crystal films in terms of the smectic elastic constants B and K and the interfacial tensions. For monomeric values of B , K and the surface tension γ (≈ 30 dyn/cm) correlations between thermally induced layer undulations decay quickly along the layer normal (typically after only a few smectic layers). Thus we interpret the diffuse scattering in Fig. 2 as arising from two independent sources of roughness: static, conformal layer undulations from the substrate, and thermally induced layer undulations. The lack of detailed information on B , K and the interfacial surface tensions for these materials as a function of monomer concentration prohibits the use of Holyst's model to calculate the correlation function in Eq. (1). Rather, we make the ansatz

$$F(q_z) e^{q_z^2 \bar{C}(x)} \equiv \int \int dz dz' \frac{d\rho(z)}{dz} \frac{d\rho(z')}{dz'} \times e^{q_z^2 C(x, z-z')} e^{-iq_z(z-z')}, \quad (2)$$

where $\bar{C}(x)$ is now a semiempirical correlation function which has been averaged over the film thickness

$$\bar{C}(x) = \bar{\sigma}^2 \exp\left(-\left|\frac{x}{\bar{\xi}_\perp}\right|^{2\bar{h}}\right). \quad (3)$$

The first term in curly brackets is the specular contribution at $q_x=0$. The remainder of the summation represents the off-specular diffuse component. Seven terms of this series were retained to describe the diffuse scattering in Fig. 2. This function was convolved with the instrument resolution. Only three parameters, \bar{h} , $\bar{\sigma}$, and $\bar{\xi}$, were varied for the fitting of each data set. These are listed in Table I. For purposes of

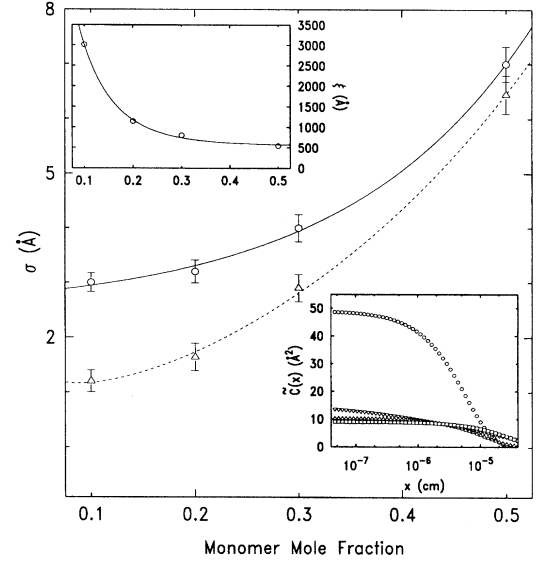


FIG. 3. Variations of $\bar{\sigma}$ (open circles) with monomer concentration. The solid line is a guide to the eye. Open triangles denote the thermal contribution to the roughness assuming a static undulation amplitude of 2.75 Å. The dashed line is a guide to the eye. Upper inset: concentration dependence of the average undulation correlation length. Lower inset: \bar{C} as a function of separation for 10% (squares), 20% (triangles), 30% (inverted triangles), and 50% (circles) films.

The function $F(q_z)$ represents a specularly reflected intensity. In the above expression, $\bar{\sigma}$ and $\bar{\xi}_\perp$ correspond to a root-mean-square layer roughness and an in-plane roughness correlation length, respectively, which have been averaged over the film. \bar{h} is an exponent which characterizes the correlation decay within the plane of the smectic layers. The functional form of Eq. (3) was chosen to be of the same form as that used previously to describe roughness in pure polymer films. This facilitates direct comparisons with the data from films studied here.

Expanding the exponential containing \bar{C} yields the following expression:

$$I(q) = \frac{1}{q_z^2} F(q_z) \left\{ 2\pi\delta(q_z) + \sum_{n=1}^{\infty} \frac{(\bar{\sigma}^2 q_z^2)^n}{n!} \int_{-\infty}^{\infty} dx e^{-n(|x|/\bar{\xi})^{2\bar{h}}} e^{-iq_x x} \right\}. \quad (4)$$

analysis, a uniform composition of monomer and polymer throughout the film is assumed.

At low monomer concentrations $\bar{\sigma}$ (Fig. 3) is very nearly equal to the roughness of the chemisorbed alkylsiloxane film, the density profile of which has been reported [4,14]. This is consistent with the existence of static roughness previously studied in pure copolymer films [4,9]. For higher monomer

concentrations $\bar{\sigma}$ shows a dramatic increase. Assuming that the static and thermal undulations are independent sources of roughness,

$$\bar{\sigma}^2 = \sigma_{\text{th}}^2 + \sigma_{\text{st}}^2. \quad (5)$$

For a smectic film with a finite thickness D_z along the layer normal [13],

$$\sigma_{\text{th}}^2 = \frac{k_B T}{4\pi\sqrt{KB}} \ln \frac{\sqrt{\lambda D_z}}{a_0}. \quad (6)$$

The number and relative intensities of the Bragg reflections for the 10% film are comparable to bulk copolymer samples, implying a polymeric value of B ($\approx 2.5 \times 10^9$ dyn/cm²) yielding $\sigma_{\text{th}} = 1.2$ Å and $\sigma_{\text{st}} = 2.75$ Å for the roughnesses of the 10% monomer mole fraction film [15]. Assuming that static roughness is constant for the four films, the thermal undulation amplitude can be determined and is plotted in Fig. 3. For the 50% film σ_{th} approaches 6.4 Å. From Eq. (4) this implies $B \approx 1 \times 10^7$ dyn/cm², which is the correct order of magnitude for a monomeric smectic-C liquid crystal.

ξ is also quite sensitive to monomer concentration, falling by nearly an order of magnitude between 10% and 50% (Fig. 3, upper inset). ξ is essentially the width of the diffuse peak, setting the in-plane length scale for the roughness correlations averaged across the film thickness. Its decrease with increasing monomer concentration is consistent with the rapid damping of the thermal layer undulation correlation function calculated by Holyst [13]. The measured correlation functions \tilde{C} for the various films are plotted in Fig. 3 (lower inset).

Microscopically, the behavior of $\bar{\sigma}$ and ξ is linked to the segregation of the siloxane backbone by the liquid-crystal mesogen. From x-ray diffraction studies of bulk samples the intermesogen separation of the pure copolymer and the monomer are both approximately 5 Å. Since the mesogen

density remains virtually unchanged, the mixtures effectively represent a decrease in siloxane concentration. To preserve the preferred monomer layer spacing, the siloxane backbones become “squeezed” out, assuming conformations which are less confined between smectic layers. This leads to a reduction in the Bragg scattering and an increase in the average layer roughness $\bar{\sigma}$. Also, the increase in the free monomer decreases the effective value of B for the films and layer undulations may be relaxed more readily by local changes in the layer spacing. Undulations will hence persist over shorter distances within and between layers yielding a lower value for the average layer undulation correlation length ξ .

As stated above, uniform compositions are assumed for each film. What we interpret as separate surface and “bulk” regions in the 50% film (Fig. 1) does not necessarily imply phase segregation, especially since none has been observed in bulk mixtures. Surface segregation or distillation may occur at film interfaces, although we have no evidence for this in our studies. Further investigations into these effects are underway.

In conclusion we have examined the crossover from static to thermally dominated roughness of smectic layers in Langmuir-Blodgett films of liquid-crystal polymer-monomer mixtures. An increase in the monomer mole fraction leads to an increase in the root-mean-square layer roughness and a decrease in the average in-plane correlation length of the layer undulation correlation function. A theoretical description of the variations of the two contributions to the smectic layer undulations with relative concentration would be of considerable interest.

The financial support of the Office of Naval Research is gratefully acknowledged. We would like to thank Dr. J. Naciri for the copolymer and monomer samples and Dr. A. F. Thibodeaux and Dr. R. S. Duran for the transfer of multilayers. One of us (R.E.G.) acknowledges support from the National Research Council.

-
- [1] See, e.g., S. Chandrasekhar, *Liquid Crystals* (Cambridge University, Cambridge, 1992), 2nd ed.
- [2] D. J. Tweet, R. Holyst, B. D. Swanson, H. Straiger, and L. B. Sorensen, *Phys. Rev. Lett.* **65**, 2157 (1990); R. Holyst, D. J. Tweet, and L. B. Sorensen, *ibid.* **65**, 2153 (1990).
- [3] R. E. Geer, S. B. Qadri, R. Shashidhar, A. F. Thibodeaux, and R. S. Duran, *Liq. Cryst.* **16**, 869 (1994).
- [4] R. E. Geer, R. Shashidhar, A. Thibodeaux, and R. Duran, *Phys. Rev. Lett.* **71**, 1391 (1993).
- [5] B. R. McClain, D. D. Lee, B. L. Carvalho, S. G. J. Mochrie, S. H. Chen, and J. D. Lister, *Phys. Rev. Lett.* **72**, 246 (1994).
- [6] I. M. Tidswell, T. A. Rabedeau, P. S. Pershan, and S. E. Kosowsky, *Phys. Rev. Lett.* **66**, 2108 (1991).
- [7] J. Naciri, S. Pfeiffer, and R. Shashidhar, *Liq. Cryst.* **10**, 585 (1991).
- [8] J. C. Ruth, J. Naciri, and R. Shashidhar, *Liq. Cryst.* **16**, 883 (1994).
- [9] R. E. Geer, S. B. Qadri, and R. Shashidhar, *Ferroelectrics* **149**, 147 (1993).
- [10] Y. Shi, B. Cull, and S. Kumar, *Phys. Rev. Lett.* **71**, 2773 (1993).
- [11] S. K. Sinha, M. K. Sanyal, A. Gibaud, S. K. Satija, C. F. Majkrzak, and H. Homma, in *Science and Technology of Nanostructured Magnetic Materials*, edited by G. C. Hadjipanayis and G. A. Prinz (Plenum, New York, 1991).
- [12] P. G. DeGennes, *The Physics of Liquid Crystals* (Oxford University, London, 1974).
- [13] R. Holyst, *Phys. Rev. A* **44**, 3692 (1991).
- [14] I. M. Tidswell, B. M. Ocko, P. S. Pershan, S. R. Wasserman, G. M. Whitesides, and J. D. Axe, *Phys. Rev. B* **41**, 1111 (1990).
- [15] The values of K and λ used in this calculation are 1×10^{-6} dynes and 2 Å, respectively.